Biochemical and Biophysical Research Communications 452 (2014) 334–339

Contents lists available at ScienceDirect

Biochemical and Biophysical Research Communications

journal homepage: www.elsevier.com/locate/ybbrc

Examining the critical roles of human CB2 receptor residues Valine 3.32 (113) and Leucine 5.41 (192) in ligand recognition and downstream signaling activities

Mohammed Alqarni [a], Kyaw Zeyar Myint [a,b], Qin Tong [a], Peng Yang [a], Patrick Bartlow [a], Lirong Wang [a], Rentian Feng [a], Xiang-Qun Xie [a,b,c,*]

[a] Department of Pharmaceutical Sciences and Computational Chemical Genomics Screening Center, School of Pharmacy, Pittsburgh, PA 15260, USA
[b] Joint Carnegie Mellon University-University of Pittsburgh Ph.D. Program, Department of Computational Biology and Structural Biology, School of Medicine, Pittsburgh, PA 15260, USA
[c] Drug Discovery Institute, University of Pittsburgh, Pittsburgh, PA 15260, USA

ARTICLE INFO

Article history:
Received 6 August 2014
Available online 19 August 2014

Keywords:
Molecular modeling
Site-directed mutagenesis
Cannabinoid receptor subtype 2 (CB2)
Cyclic adenosine monophosphate (cAMP)
Time-resolved fluorescence resonance energy (TR-FRET) transfer
Adenylyl cyclase (AC activity)

ABSTRACT

We performed molecular modeling and docking to predict a putative binding pocket and associated ligand–receptor interactions for human cannabinoid receptor 2 (CB2). Our data showed that two hydrophobic residues came in close contact with three structurally distinct CB2 ligands: CP-55,940, SR144528 and XIE95-26. Site-directed mutagenesis experiments and subsequent functional assays implicated the roles of Valine residue at position 3.32 (V113) and Leucine residue at position 5.41 (L192) in the ligand binding function and downstream signaling activities of the CB2 receptor. Four different point mutations were introduced to the wild type CB2 receptor: V113E, V113L, L192S and L192A. Our results showed that mutation of Val113 with a Glutamic acid and Leu192 with a Serine led to the complete loss of CB2 ligand binding as well as downstream signaling activities. Substitution of these residues with those that have similar hydrophobic side chains such as Leucine (V113L) and Alanine (L192A), however, allowed CB2 to retain both its ligand binding and signaling functions. Our modeling results validated by competition binding and site-directed mutagenesis experiments suggest that residues V113 and L192 play important roles in ligand binding and downstream signaling transduction of the CB2 receptor.

1. Introduction

Cannabinoid receptors are in the Rhodopsin-like family of G-protein-coupled receptors (GPCRs), with seven characteristic hydrophobic transmembrane helices attached by three intracellular and three extracellular loops [1]. Two types of cannabinoid receptors, CB1 and CB2, were characterized and cloned in 1990 and 1993 respectively [2,3]. CB1 receptor is expressed in the central nervous system (CNS) and is less predominant in peripheral organs and tissues such as the heart, lung, the adrenal gland tonsils, and spleen [4]. Unlike CB1 receptor, CB2 receptor is predominantly expressed in the peripheral immune system such as in the spleen and lymph nodes. [3]. Such distribution pattern of CB2 receptor in the peripheral organ suggests that CB2 receptor play a crucial role in the regulation of the immune response [5]. Therefore, CB2-selective ligands may likely hold promise for the treatment of diseases with immune origin, e.g. chronic pain [6], osteoporosis [7] and various cancers such as lung, bladder [8], pancreas [9], breast [10] and prostate [11] without CNS-mediated psychoactive effects. Cannabinoid agonist binding elicits a series of conformational changes among the transmembrane helices that shift the equilibrium toward the active receptor state [12]. Consequently, $G\alpha_i$, a family of G proteins, binds to third intracellular loop and C-terminus of CB2 to inhibit forskolin-stimulated adenylyl cyclase (reduction in cAMP levels), activate the mitogen-activated protein kinase (MAPK) cascade and regulate protein kinase A (PKA) phosphorylation, all of which are important in maintaining cell function integrity [13]. Moreover, activation of the CB2 receptor turns to initiate a transient Ca^{2+} signaling elevation in endothelial cells by endocannabinoid anandamide [14].

Due to the difficulties in GPCR functional expression and purification as well as their inherent flexibility, only a limited GPCR crystal structures have been elucidated to date [15]. Given the scarcity of GPCR crystal structures, generation of 3D models derived from

* Corresponding author at: 3501 Terrace Street, 529 Salk Hall, University of Pittsburgh, Pittsburgh, PA 15260, USA.
E-mail address: xix15@pitt.edu (X.-Q. Xie).

http://dx.doi.org/10.1016/j.bbrc.2014.08.048
0006-291X/

alignment with previously reported GPCR structures and complementary site-directed mutagenesis experiments are considered to be a feasible alternative method to study ligand binding and receptor activation [16].

Several CB2 binding pocket residues have been confirmed for their importance in agonist and antagonist binding, such as S112, W172, Y190, W194, F197, W258, and S285 [17–24]. Moreover, since the third and fifth transmembrane regions of CB2 receptor are playing curial roles in the binding of the vast majority of cannabinoid ligands and consequent signal transduction [17,25], we investigated the possible roles of V113 of TM3 (position 3.32) and L192 of TM5 (position 5.41) in binding with three structurally diverse CB2 ligands: CP-55,940, a non-classical cannabinoids agonist; SR144528, a diarylpyrazole inverse agonist; and XIE95-26, a biamide derivative inverse agonist [26] (Supplemental Fig. 1).

2. Materials and methods

2.1. Molecular modeling

A CB2 homology model was constructed from the antagonist-bound A2A receptor (3EML.pdb) [27], human dopamine D3 receptor (3PBL.pdb) [28], bovine rhodopsin (1L9H.pdb and 1F88.pdb) [29,30], human beta2-adrenergic receptor (2RH1.pdb) [31], and the turkey beta1-adrenergic receptor (2Y00.pdb and 2VT4.pdb) [32,33] using the I-TASSER protein structure prediction server [34]. Five models were obtained after such prediction, and the model (model 1) with the highest C-score (-0.96) was selected as the final model. It was further minimized using a conjugate gradient method with the AMBER force field (AMBER7 FF99) defined in the Tripos Sybyl software [35]. The minimization was run for 500 iterations and the maximum derivative of energy was set to 0.05 kcal mol^{-1} $Å^{-1}$. MOLCAD analysis [35] was performed on the 3D homology model to find a solvent-accessible cavity around important agonist and inverse agonist binding residues (Fig. 1A). In addition, two residues, namely V3.32 (V113) and L5.41 (L192), displays hydrophobic interactions with all three ligands during the simulation. In order to validate these findings, we performed site-directed mutagenesis experiments and functional assays. CB2 ligands CP-55,940, SR144528 and XIE95-26 were docked into the putative pocket. The docking mode was GeomX and other default docking parameters defined in the Surflex-Dock module as previously described [36,37].

2.2. Mutagenesis experiments

Mutation of the CB2 receptor was carried out using the QuikChange site-directed mutagenesis kit (QuikChange; Stratagene, CA) according to the manufacturer's recommendations. A point mutation was performed individually to the human CB2 expression plasmid pcDNA3.1 + 3X – HA-hCB2 (Missouri S&T cDNA Resources Center), which was used as a template. The mixture was transformed into XL10-Gold ultracompetent cells (QuikChange; Stratagene, CA). The mutant CB2 plasmids were subsequently confirmed by DNA sequencing.

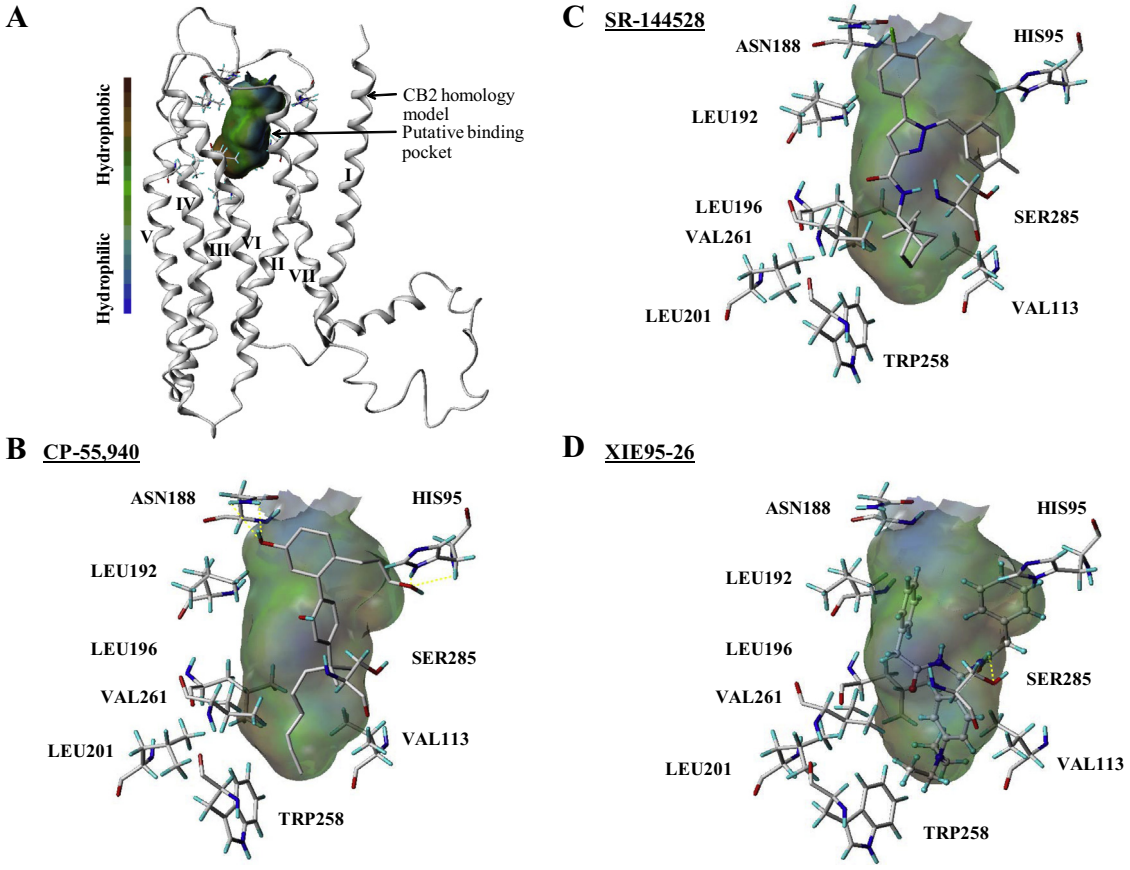

Fig. 1. Molecular docking of CB2 ligands into putative CB2 binding site. (A) 3D homology model of the CB2 seven transmembrane helices showing amphipathic-binding cavity, lipophilicity scale is used to colored the pocket in which hydrophobic areas are shown in brown and hydrophilic areas are in blue. (B–D) Interactions between each ligand and the receptor. Magnified views of the predicted binding pocket, which show hydrophobic residues such as L201, V261, V113, L192 showed interact with CP-55,940, SR144528 and XIE95-26. In addition, N188 reveal H-bond with both CP-55,940 and SR144528. (For interpretation of the references to color in this figure legend, the reader is referred to the web version of this article.)

2.3. Transfection and cell culture

The transfection was performed to the Chinese Hamster Ovary (CHO) cells (90% confluence) in 60-mm culture plates according to manufacturer's protocol (Invitrogen). 8.0 μg of mutated human CB2 receptor plasmid and 20 μL of the transfection agent Lipofectamine 2000 were diluted in 1 mL of Opti-MEM reduced serum medium, mixed, incubated for 20 min at room temperature, and then added to the cell culture. After 4 h of transfection, the medium was refreshed and the cells were incubated for 24 h. The transfected cells were selected by conditional incubation in presence of 800 μg/mL G-418 (Gibco) for 5 days. The selected cells were then maintained in the medium containing 220 μg/mL of G-418.

2.4. Cell harvesting and membrane preparation

The plates containing high confluent of mutants transfected Chinese Hamster Ovary (CHO) cells were rinsed twice with phosphate-buffered saline pH 7.5 (PBS) before scraping the plates. Then the attached cells were collected by scraping the plates and centrifuge at 500*g* for 5 min at 4 °C. The cell pellets were resuspended in 5 mL of membrane preparation buffer (50 mM Tris–HCl pH 7.4, 5 mM $MgCl_2$, 2.5 mM EGTA and 200 mM sucrose) and homogenized with a Polytron Homogenizer (Kinematica, Littau-Lucerne, Switzerland). The lysed cells were centrifuged at 500*g* for 5 min at 4 °C and the supernatant was collected. The remaining pellets were resuspended in membrane buffer and centrifuged again for three times. All supernatants were combined and centrifuged at 68,000*g* for 90 min at 4 °C. Pellets were then collected and resuspended in membrane preparation buffer for competition binding assays.

2.5. Western Blot analysis

Cells were lysed in RIPA buffer (Thermo, NP 89901) and protease inhibitory cocktail (Thermo Scientific, P1861281), and centrifuged at 13,000*g* for 15 min at 4 °C. Supernatants were collected and protein concentrations were determined using the BCA protein assay kit (Pierce, Rockford, IL). Each sample (25 μg each) was prepared, separated on a 10% SDS–PAGE gel and transferred onto polyvinylidene difluoride membranes (PVDF). The membrane then was blocked with 0.1% Tween 20 in PBS (PBS-T) containing 5% non-fat dried milk for 1 h and incubated in a solution of primary antibody (goat polyclonal antibody; Thermo Scientific, PA5-18428) for 1 h at room temperature. After 3 washes with PBS-T for 10 min, the membrane was incubated in secondary antibody solution (Santa Cruz Biotechnology, Santa Cruz, CA) for 1 h at room temperature. The membrane was detected using Western Blotting Detection Reagents (Super Signal West Femto, Thermo Scientific).

2.6. Competition binding assay

The protein concentration was measured using Pierce BCA Protein Assay (Rockford, IL). Three structurally distinct, representative cannabinoid ligands are CP-55,940 (CB agonist) and SR144528 (inverse agonist) were obtained from RTI International (Research Triangle Park, NC) and XIE95-26 (inverse agonist) [26]. The ligand binding was performed as previously described with little modifications [38]. Briefly, non-radioactive ligands were diluted in membrane preparation buffer, supplemented with 10% dimethyl sulfoxide and 0.4% methyl cellulose. Each assay plate well contained a total of 200 μL of reaction mixture of 5 μg of membrane protein, 3 nM of labeled [^{3}H]-CP-55,940 and unlabeled 3 ligands. Plates were incubated at 30 °C for 1 h. The reaction was terminated by rapid filtration through Unifilter GF/B filter plates using a Unifilter Cell Harvester (PerkinElmer, NL). After the plate was allowed to dry overnight, 30 μL of MicroScint-0 cocktail (PerkinElmer) was added to each well and the radioactivity was counted by PerkinElmer TopCounter. All assays were performed triplicate in duplicate wells and data are represented as the mean ± S.E.M. Bound radioactivity data was analyzed via GraphPad Prism 5.0 software.

2.7. cAMP assay

LANCE cAMP 384 kit (Perkin Elmer, Bridgeville), was used to detect cAMP as previously described [20]. Briefly, CB2 wild type and mutants transfected CHO cells were seeded in a 384-well (Perkin Elmer, Bridgeville) with a density of 2500 cells per well in 5 μL of RPMI-1640 medium. After culture overnight, stimulation buffer (DPBS 1×, containing 0.1% BSA) contains of cAMP antibody and RO20-1724 was added to each well, followed by addition of CP-55,940 (various concentration) in 5 μM forskolin stimulation buffer for agonist-inhibited adenylyl cyclase activity. The fluorescence was detected with a Synergy H1 hybrid reader (BioTek, Winooski, VT) at 340 nm excitation/665 nm emission. Each cAMP determination was averaged from at least three independent experiments, each in triplicate. EC_{50} values were calculated by nonlinear regression, dose–response curves GraphPad Prism 5.

3. Results

3.1. Homology modeling and molecular docking

As shown in (Fig. 1A), a putative binding pocket of the minimized CB2 model was found among residues pertaining to helices II, III, V, VI and VII. All compounds were docked to the binding pocket using the Surflex-Dock module [35]. The molecular docking results for CP-55,940, SR144528 and XIE95-26 were shown in (Fig. 1B–D), respectively. Several important interactions were observed for each ligand. For examples: N188 and S285 reveals H-bonding with CP-55,940 and XIE95-26 respectively and V113, L192, L201 and V261 have shown hydrophobic interactions with ligands. We have subjected these residues for site-directed mutagenesis to elucidate the importance of these residues for their role in the binding and function of the receptor. We also compared the binding modes between agonist and antagonists. Hydrophilic interactions between the CB2 model and agonist (CP-55,940) were found in the top of the binding pocket, while hydrophilic interactions between CB2 and antagonists were found in the bottom (or middle) of the binding pocket. H95 and N188 formed hydrogen bonds with CP-55,940, while these two residues only formed hydrophobic interactions with inverse agonists. Moreover, S285 formed hydrogen bonds both with SR144528 (3.5–4.7 Å) and XIE95-26 (within 3 Å). However, only hydrophobic interactions were observed between S285 and CP-55,940. In addition, we found that XIE95-26 had closer interactions with W258 compared with that of SR144528.

3.2. Expression of recombinant human wild type and mutant CB2 in CHO cells

The expression of wild-type human CB2 and V113E/L, and L192S/A mutants by stably transfected CHO cell lines was analyzed and confirmed by Western Blot (Fig. 2). The CB2 receptor is shown as the band corresponding to 41 kDa.

3.3. Ligand binding of wild type and mutant CB2 receptors

The ligand binding affinity of wild-type and mutant CB2 receptors were determined by competitive binding assays using radioactive [^{3}H]-CP-55,940 and three non-radioactive ligands. Binding

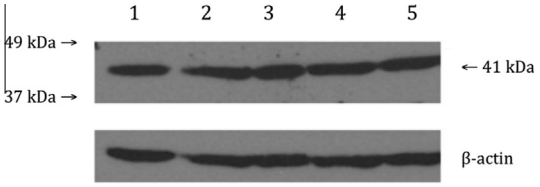

Fig. 2. Western Blot analysis of wild-type and mutant h-CB2 receptor isoforms in transfected CHO cells. From left to right: 1 – CB2 WT (wild-type), 2 – V113E, 3 – V113L, 4 – L192S, and 5 – L192A.

Table 1
Binding affinities (K_i, nM) of ligands to cannabinoid receptors of wild type and mutant CB2 stably expressed in CHO cells.

Receptors	WT	V113E	V113L	L192A	L192S
CP55,940	2.6 (1.3–5.1)[a]	ND	3.8 (0.3–46)[a]	2.3 (0.7–7.1)[a]	ND
SR144528	1.0 (0.5–1.8)[a]	ND	6.1 (2.8–12)[a]	4.8 (2.3–9.9)[a]	ND
XIE95-26	154 (43–543)[a]	ND	141 (20–972)[a]	6.1 (2.8–12)[a]	ND

[a] Data are the means and corresponding 95% confidence intervals of two independent experiments each performed in duplicate. WT: wild type; V113E, V113L, L192A and L192S: mutant human CB2; ND: binding not detected.

data (Fig. 3, summarized in Table 1) indicated that the L192A substitution had no effect on CB2's affinity for CP-55,940; whereas the binding affinities of SR144528 and XIE95-26 were slightly reduced compared to the wild-type. Similarly, the V113L substitution resulted in a slight reduction in CB2 affinity for SR144528, yet no significant effect was observed for CP-55,940 or XIE95-26 binding. Substitutions at V113E and L192S independently resulted in the complete loss of binding affinity for each of the three ligands used.

3.4. Agonist-induced inhibition of cAMP production

LANCE cAMP is time-resolved fluorescence resonance energy transfer (TR-FRET) immunoassay used to detect the signal from CHO cells stably expressing wild type CB2 and four mutant receptors. CP-55,940 was used as an agonist to induce inhibition of cAMP production in the presence of 5 μM forskolin and phosphodiesterase inhibitor RO20-1724 (50 μM). When the agonist concentration was increased, the inhibition on the forskolin-induced cAMP production also increased, resulting in an enhancement of the LANCE signal, which is inversely proportional to the concentration of cAMP. These results were congruent with the ligand–receptor binding affinity data. EC_{50} values were 32, 9.7 and 0.14 nM for wild-CB2, V113L and L192A, respectively. Further, V113E and L192S substitutions resulted in a complete loss of signal transduction (Fig. 4).

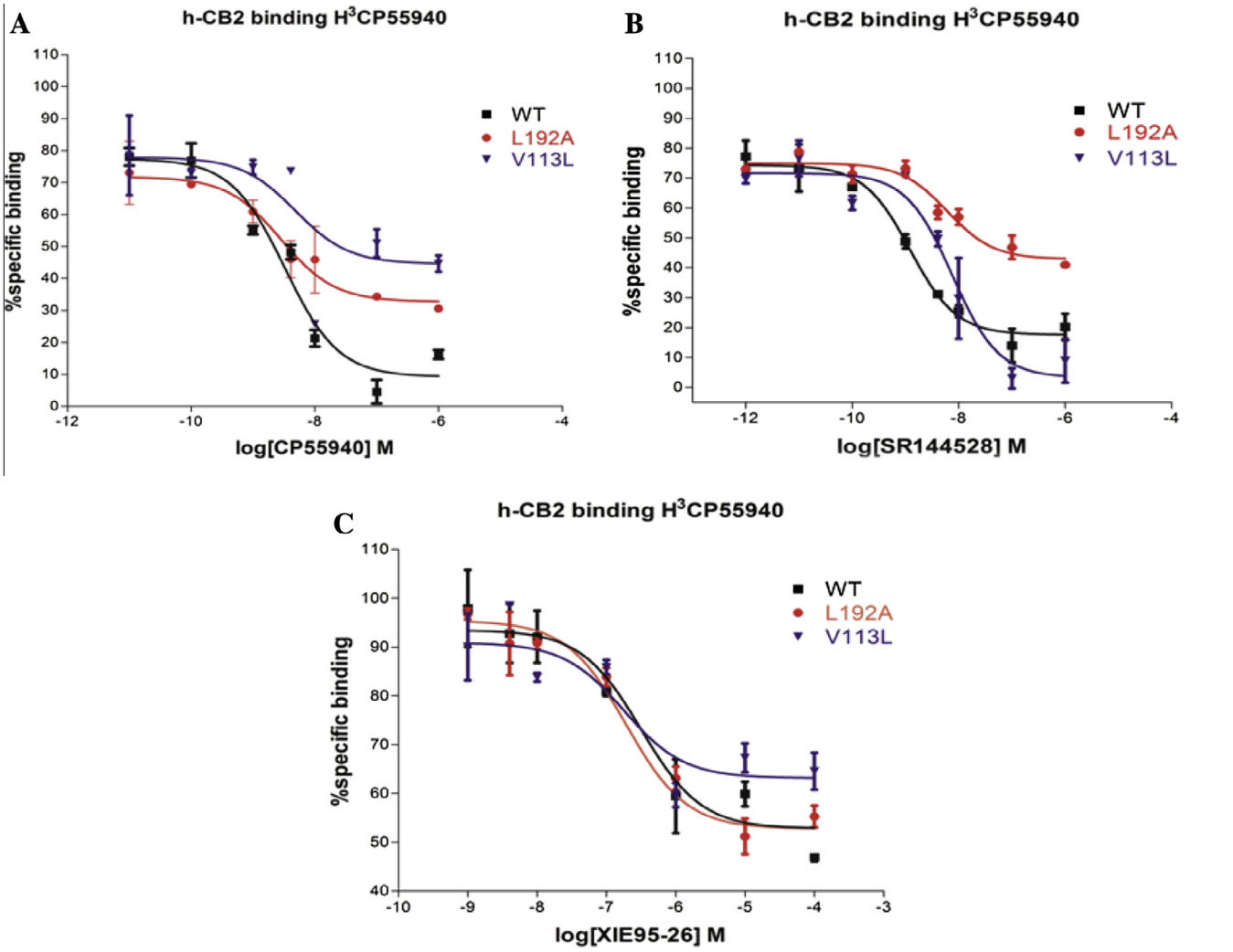

Fig. 3. Competition binding assay for wild-type CB2 (■) and mutants receptors, CB2 V113L (▼), L192A (●) binding to (A. CP-55,940; B. SR144528; C. XIE95-26). The assays were performed on membranes prepared from CHO cell line stably expressing wild-type or mutants human CB2receptors. Data are mean ± S.E.M. of two independent experiments performed in duplicate. Curves were generated using GraphPad Prism 5.

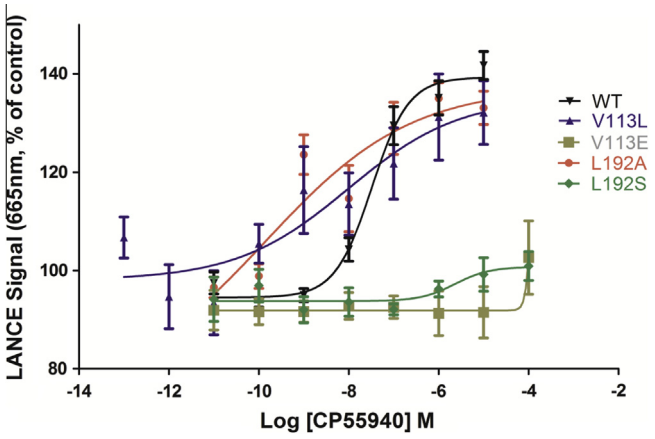

Fig. 4. Agonist-induced inhibition of forskolin-stimulated cAMP accumulation of CB2 WT and all mutants' receptors. (▼) WT- CB2, (▲) V113L, (■) V113E (●) L192A and (♦) L192S. All receptors were stably expressed in CHO cells. Data are mean ± S.E.M. of at least three independent experiments in triplicate.

4. Discussion

Molecular modeling and mutagenesis experiments were applied to gain valuable insights into the effect of certain CB2 residues on receptor binding with agonists and antagonists. A 3D homology model of CB2 was first constructed and then further minimized using a conjugate gradient method. The minimized model served as the basis for molecular docking studies (see Materials and Methods). A putative binding pocket was first predicted via the MOLCAD analysis, which suggested the importance of several aromatic and polar residues that have previously been validated experimentally [17–24]. As shown in (Fig. 1A), the putative binding pocket was amphipathic and composed of hydrophilic and electrically charged residues, such as N188 and H95 near the upper part of the pocket facing the extracellular loop 2 (ECL-2) and hydrophobic residues such as V113, L201, V261 and W258 near the bottom of the pocket. These results were found to be congruent with previously studies, which also suggested a hydrophobic binding pocket [36,37].

Results of molecular docking with the CP-55,940, SR144528 and XIE95-26 ligands were shown in (Fig. 1B–D), revealing several important ligand–receptor interactions for each ligand. Specifically, five hydrophobic residues were found to be in close contact with all three ligands during docking simulations: V113, L192, L201, V261 and W258. Indeed, L201, V261 and W258 have previously been implicated in the formation of the ligand binding pocket [23,39]. A prior report affirms that residue 3.32 is occupied by a negatively charged amino acid in biogenic amine receptors (D2 Dopamine, ß2 Adrenergic and m3 Muscarinic) and that it is essential for recognition and binding of endogenous amines [40]. In an attempt to resemble the functionality of this residue in amine receptors [41], substituted endogenous V83 (position 3.32) with Aspartic acid (D) in the A2a adenosine receptor. The V83D mutant of A2a adenosine receptor lead to loss bind to any ligands tested. Interestingly, substitution of the same Valine residue with Leucine (V83L) did not significantly affect binding with any ligand as same as the wild-type A2a adenosine receptor. Using a similar approach, with the CB2 receptor, the V113E substitution led to the complete loss of binding for CB2 ligands and the elimination of receptor downstream signaling activities, whereas, the V113L isoform displayed specific binding activity that was comparable to wild-type CB2. Molecular docking analyses showed that V113 maintains hydrophobic interactions with the alkyl chain of CP-55,940, the fenchyl (bulky) group of SR144528 and an aromatic ring of XIE95-26 at distances of 3.27, 3.33 and 3.04 Å, respectively. Similarly, side chain of L192 makes hydrophobic interaction with CP-55,940, SR144528 and XIE95-26 at distances of 3.80, 3.25 and 4.64 Å, respectively. In order to validate the modeling studies, these two residues were subjected to mutagenesis experiments to elucidate the role of hydrophobic interaction with both agonist and inverse agonist. Mutation of V113 to E and L192 to S amino acid interrupted the hydrophobic interactions with the ligands and all three ligands lost the binding (Table 1). However, reintroducing the hydrophobic feature via L192A and V113L mutants restored the binding of CP-55,940, SR144528 and XIE95-26 to the CB2 receptor. In fact, L192A and V113L mutants showed only 5-fold and 6-fold reduction for SR144528 binding and almost no significant change for CP-55,940 and XIE95-26 binding (Table 1). These results confirmed that our predicted residues play an important role in CB2 ligand binding.

The following functional experiments further verified the importance of the predicted residues: V113 and L192. In a cell-based cyclase assay, an agonist will activate CB2 receptor, cause the dissociation of $G\alpha_i$ and inhibit forskolin-induced AC activity, resulting in the decreased cAMP and an increased LANCE signal [42]. As shown in Fig. 4, there is no inhibition of cAMP accumulation mediated by CP-55,940 in the V113E and L192S mutant cells. However, mutating to different hydrophobic residues restored the functionality of the receptor as shown by the mutants V113L and L192A. The EC_{50} values of CP-55,940 on the WT, V113L and L192A were 32, 9.7 and 0.14 nM, respectively. These results indicated that hydrophobic residues at positions 3.32 (V113) and 5.41 (L192) are important for both ligand–receptor interaction and function of the receptor CB2.

Conflict of interest

The authors declare no conflict of interests.

Acknowledgment

This project is supported by grants from NIH (NIH R01 DA025612, P30 DA035778 and P30 CA047904).

Appendix A. Supplementary data

Supplementary data associated with this article can be found, in the online version, at http://dx.doi.org/10.1016/j.bbrc.2014.08.048.

References

[1] J.M. Baldwin, The probable arrangement of the helices in G protein-coupled receptors, EMBO J. 12 (1993) 1693–1703.
[2] L.A. Matsuda, S.J. Lolait, M.J. Brownstein, A.C. Young, T.I. Bonner, Structure of a cannabinoid receptor and functional expression of the cloned cDNA, Nature 346 (1990) 561.
[3] S. Munro, K.L. Thomas, M. Abu-Shaar, Molecular characterization of a peripheral receptor for cannabinoids, Nature 365 (1993) 61.
[4] N.E. Kaminski, M.E. Abood, F.K. Kessler, B.R. Martin, A.R. Schatz, Identification of a functionally relevant cannabinoid receptor on mouse spleen cells that is involved in cannabinoid-mediated immune modulation, Mol. Pharmacol. 42 (1992) 736–742.
[5] I. Racz, X. Nadal, J. Alferink, J.E. Banos, J. Rehnelt, M. Martin, et al., Crucial role of CB(2) cannabinoid receptor in the regulation of central immune responses during neuropathic pain, J. Neurosci. 28 (2008) 12125–12135.
[6] E.C. Mbvundula, K.D. Rainsford, R.A. Bunning, Cannabinoids in pain and inflammation, Inflammopharmacology 12 (2004) 99–114.
[7] M. Karsak, M. Cohen-Solal, J. Freudenberg, A. Ostertag, C. Morieux, U. Kornak, et al., Cannabinoid receptor type 2 gene is associated with human osteoporosis, Hum. Mol. Genet. 14 (2005) 3389–3396.
[8] S. Hart, O.M. Fischer, A. Ullrich, Cannabinoids induce cancer cell proliferation via tumor necrosis factor alpha-converting enzyme (TACE/ADAM17)-mediated transactivation of the epidermal growth factor receptor, Cancer Res. 64 (2004) 1943–1950.

[9] C. Blazquez, A. Carracedo, L. Barrado, P.J. Real, J.L. Fernandez-Luna, G. Velasco, et al., Cannabinoid receptors as novel targets for the treatment of melanoma, FASEB J. 20 (2006) 2633–2635.
[10] L. De Petrocellis, D. Melck, A. Palmisano, T. Bisogno, C. Laezza, M. Bifulco, et al., The endogenous cannabinoid anandamide inhibits human breast cancer cell proliferation, Proc. Natl. Acad. Sci. U.S.A. 95 (1998) 8375–8380.
[11] D. Melck, L. De Petrocellis, P. Orlando, T. Bisogno, C. Laezza, M. Bifulco, et al., Suppression of nerve growth factor Trk receptors and prolactin receptors by endocannabinoids leads to inhibition of human breast and prostate cancer cell proliferation, Endocrinology 141 (2000) 118–126.
[12] G. Milligan, R.A. Bond, Inverse agonism and the regulation of receptor number, Trends Pharmacol. Sci. 18 (1997) 468–474.
[13] D.G. Demuth, A. Molleman, Cannabinoid signalling, Life Sci. 78 (2006) 549–563.
[14] C. Zoratti, D. Kipmen-Korgun, K. Osibow, R. Malli, W.F. Graier, Anandamide initiates Ca(2+) signaling via CB2 receptor linked to phospholipase C in calf pulmonary endothelial cells, Br. J. Pharmacol. 140 (2003) 1351–1362.
[15] B. Kobilka, G.F. Schertler, New G-protein-coupled receptor crystal structures: insights and limitations, Trends Pharmacol. Sci. 29 (2008) 79–83.
[16] S. Ortega-Gutierrez, M.L. Lopez-Rodriguez, CB1 and CB2 cannabinoid receptor binding studies based on modeling and mutagenesis approaches, Mini Rev. Med. Chem. 5 (2005) 651–658.
[17] Q. Tao, S.D. McAllister, J. Andreassi, K.W. Nowell, G.A. Cabral, D.P. Hurst, et al., Role of a conserved lysine residue in the peripheral cannabinoid receptor (CB2): evidence for subtype specificity, Mol. Pharmacol. 55 (1999) 605–613.
[18] M.H. Rhee, I. Nevo, M.L. Bayewitch, O. Zagoory, Z. Vogel, Functional role of tryptophan residues in the fourth transmembrane domain of the CB(2) cannabinoid receptor, J. Neurochem. 75 (2000) 2485–2491.
[19] S.D. McAllister, Q. Tao, J. Barnett-Norris, K. Buehner, D.P. Hurst, F. Guarnieri, et al., A critical role for a tyrosine residue in the cannabinoid receptors for ligand recognition, Biochem. Pharmacol. 63 (2002) 2121–2136.
[20] Y. Zhang, Z. Xie, L. Wang, B. Schreiter, J.S. Lazo, J. Gertsch, et al., Mutagenesis and computer modeling studies of a GPCR conserved residue W5.43(194) in ligand recognition and signal transduction for CB2 receptor, Int. Immunopharmacol. 11 (2011) 1303–1310.
[21] Z.H. Song, C.A. Slowey, D.P. Hurst, P.H. Reggio, The difference between the CB(1) and CB(2) cannabinoid receptors at position 5.46 is crucial for the selectivity of WIN55212-2 for CB(2), Mol. Pharmacol. 56 (1999) 834–840.
[22] Q. Tao, M.E. Abood, Mutation of a highly conserved aspartate residue in the second transmembrane domain of the cannabinoid receptors, CB1 and CB2, disrupts G-protein coupling, J. Pharmacol. Exp. Ther. 285 (1998) 651–658.
[23] N.M. Nebane, D.P. Hurst, C.A. Carrasquer, Z. Qiao, P.H. Reggio, Z.H. Song, Residues accessible in the binding-site crevice of transmembrane helix 6 of the CB2 cannabinoid receptor, Biochemistry 47 (2008) 13811–13821.
[24] M.H. Rhee, Functional role of serine residues of transmembrane dopamin VII in signal transduction of CB2 cannabinoid receptor, J. Vet. Sci. 3 (2002) 185–191.
[25] D. Shire, B. Calandra, M. Bouaboula, F. Barth, M. Rinaldi-Carmona, P. Casellas, et al., Cannabinoid receptor interactions with the antagonists SR 141716A and SR 144528, Life Sci. 65 (1999) 627–635.
[26] P. Yang, K.Z. Myint, Q. Tong, R. Feng, H. Cao, A.A. Almehizia, et al., Lead discovery, chemistry optimization, and biological evaluation studies of novel biamide derivatives as CB(2) receptor inverse agonists and osteoclast inhibitors, J. Med. Chem. 55 (22) (2012) 9973–9987.
[27] V.-P. Jaakola, M.T. Griffith, M.A. Hanson, V. Cherezov, E.Y.T. Chien, J.R. Lane, et al., The 2.6 angstrom crystal structure of a human A2A adenosine receptor bound to an antagonist, Science 322 (2008) 1211–1217.
[28] E.Y.T. Chien, W. Liu, Q. Zhao, V. Katritch, G. Won Han, M.A. Hanson, et al., Structure of the human dopamine d3 receptor in complex with a D2/D3 selective antagonist, Science 330 (2010) 1091–1095.
[29] T. Okada, Y. Fujiyoshi, M. Silow, J. Navarro, E.M. Landau, Y. Shichida, Functional role of internal water molecules in rhodopsin revealed by X-ray crystallography, Proc. Natl. Acad. Sci. 99 (2002) 5982–5987.
[30] K. Palczewski, T. Kumasaka, T. Hori, C.A. Behnke, H. Motoshima, B.A. Fox, et al., Crystal structure of rhodopsin: a G protein-coupled receptor, Science 289 (2000) 739–745.
[31] V. Cherezov, D.M. Rosenbaum, M.A. Hanson, S.G. Rasmussen, F.S. Thian, T.S. Kobilka, et al., High-resolution crystal structure of an engineered human beta2-adrenergic G protein-coupled receptor, Science 318 (2007) 1258–1265.
[32] T. Warne, R. Moukhametzianov, J.G. Baker, R. Nehme, P.C. Edwards, A.G.W. Leslie, et al., The structural basis for agonist and partial agonist action on a [bgr]1-adrenergic receptor, Nature 469 (2011) 241–244.
[33] T. Warne, M.J. Serrano-Vega, J.G. Baker, R. Moukhametzianov, P.C. Edwards, R. Henderson, et al., Structure of a beta1-adrenergic G-protein-coupled receptor, Nature 454 (2008) 486.
[34] A. Roy, A. Kucukural, Y. Zhang, I-TASSER: a unified platform for automated protein structure and function prediction, Nat. Protoc. 5 (2010) 725.
[35] SYBYL-X 1.2. 1699 South Hanley Rd., St. Louis, Missouri, 63144, USA.
[36] J.Z. Chen, J. Wang, X.Q. Xie, GPCR structure-based virtual screening approach for CB2 antagonist search, J. Chem. Inf. Model. 47 (2007) 1626–1637.
[37] X.Q. Xie, J.Z. Chen, E.M. Billings, 3D structural model of the G-protein-coupled cannabinoid CB2 receptor, Proteins 53 (2003) 307–319.
[38] C.A. Lunn, J.S. Fine, A. Rojas-Triana, J.V. Jackson, X. Fan, T.T. Kung, et al., A novel cannabinoid peripheral cannabinoid receptor-selective inverse agonist blocks leukocyte recruitment in vivo, J. Pharmacol. Exp. Ther. 316 (2006) 780–788.
[39] P. Gouldson, B. Calandra, P. Legoux, A. Kerneis, M. Rinaldi-Carmona, F. Barth, et al., Mutational analysis and molecular modelling of the antagonist SR 144528 binding site on the human cannabinoid CB(2) receptor, Eur. J. Pharmacol. 401 (2000) 17–25.
[40] A.M. van Rhee, K.A. Jacobson, Molecular architecture of G protein-coupled receptors, Drug Dev. Res. 37 (1996) 1–38.
[41] Q. Jiang, B.X. Lee, M. Glashofer, A.M. van Rhee, K.A. Jacobson, Mutagenesis reveals structure-activity parallels between human A2A adenosine receptor and biogenic amine G protein-coupled receptor, J. Med. Chem. 40 (1997) 2588–2595.
[42] M.H. Rhee, M. Bayewitch, T. Avidor-Reiss, R. Levy, Z. Vogel, Cannabinoid receptor activation differentially regulates the various adenylyl cyclase isozymes, J. Neurochem. 71 (1998) 1525–1534.